Optimal Utility of Vehicles in LTE-V Scenario: An Immune Clone-Based Spectrum Allocation Approach

Quyuan Luo, *Student Member, IEEE*, Changle Li, *Senior Member, IEEE*, Tom H. Luan, *Member, IEEE*, and Yingyou Wen

***Abstract*— With the surge service requirements from vehicular users, especially for automated driving, providing real-time high-rate wireless connections to fast-moving vehicles is ever demanding. This motivates the development of the emerging LTE-V network, a 5G cellular-based vehicular technology. However, note that the vehicular user group is typically of a very large scale, whereas the bandwidth spectrum available for vehicular communications is very limited. To efficiently allocate and utilize the slim spectrum resource to vehicle users are therefore important. This paper develops a service priority oriented spectrum allocation scheme in an LTE-V network, which explores the features of vehicular networks toward economic yet QoS guaranteed spectrum allocation. Specifically, the work exploits two features of the vehicular networks. First, vehicles in the proximity typically have similar information requirements, e.g., road conditions. As a result, the location-based multicast (i.e., geocast) could be applied to save the spectrum. Second, different types of vehicles, e.g., ambulances, buses, and private cars, are of different bandwidth and service requirements. Therefore, differential services and spectrum allocations should be applied. By jointly considering the above features, we develop a 2-D service importance oriented framework for LTE-V network spectrum allocations. The spectrum allocation issue is finally modeled as a mixed integer programming problem to maximize the system utility, and solved using an immune clonal based algorithm. The convergence of the proposed algorithm is proved, and using numerical results, we show that our proposal can outperform the typical heuristics-based spectrum resource allocation in terms of convergence and average delay.**

***Index Terms*— Vehicular communication, LTE-V, spectrum resource allocation, service importance evaluation, graph coloring model, immune clonal.**

Manuscript received October 9, 2017; revised March 15, 2018; accepted June 5, 2018. Date of publication July 26, 2018; date of current version May 1, 2019. This work was supported in part by the National Natural Science Foundation of China under Grant 61571350 and Grant 61601344, in part by the Key Research and Development Program of Shaanxi under Grant 2017KW-004, Grant 2017ZDXM-GY-022, and Grant 2018ZDXM-GY-038, and in part by the 111 Project under Grant B08038. The Associate Editor for this paper was C. F. Mecklenbräuker. *(Corresponding author: Changle Li.)*

Q. Luo and C. Li are with the State Key Laboratory of Integrated Services Networks, Xidian University, Xi'an 710071, China (e-mail: clli@mail.xidian.edu.cn).

T. H. Luan is with the School of Cyber Engineering, Xidian University, Xi'an 710071, China.

Y. Wen is with the School of Computer Science and Engineering, Northeastern University, Shenyang 110819, China, and also with the State Key Laboratory of Software Architecture, Northeastern University, Shenyang 110179, China.

Digital Object Identifier 10.1109/TITS.2018.2850311

I. Introduction

AS PREDICTED, by 2020 the worldwide mobile traffic alone will increase by 33 times as compared to that of the 2010 figures [1], [2]. A great portion of traffic could be contributed by the vehicular users, especially with the emerging automated driving and media-rich vehicular infotainment applications [3]. To enable the ubiquitous connections to vehicles, the cellular based approach is still the most scalable and practical approach, which motivates the emerging LTE-Vehicle (LTE-V) networks [4]–[6].

LTE-based V2X was widely used as LTE-V in the Chinese vehicular communications industry [7]. LTE-V technology, considered to be one of the optimal choices for effective Intelligent Transportation System (ITS) is widely acknowledged by automobile manufacturers, vendors of automobile technologies and parts, vendors of communication solutions, and telecom operators. Compared with other ITS solutions, LTE-V technology features low cost and rapid deployment since it can fully utilize existing base stations around the world [8], as well as providing V2I communications because of its high data rate, high penetration rate, comprehensive QoS supporting, and large coverage. Due to the limited spectrum resource yet the large population of vehicles, a key issue in LTE-V networks is how to efficiently allocate the precious spectrum resources to meet the service requirements of vehicles [9]. Chen *et al.* [10] develop an optimal packet schedule to allocate the resource and formulate the problem as an integer linear program (ILP). Li *et al.* [11] study joint congest control and resource optimization to explore the energy efficiency (EE)-guaranteed trade-off between throughput utility and delay performance, and formulate the considered problem as a stochastic optimization problem. To meet the service requirements of ITS, Zheng *et al.* [12] propose an optimal computation resource allocation scheme to maximize the total long-term expected reward of the vehicular cloud computing (VCC) system by taking advantage of the cloud computing technique.

Since the vehicular user group are of a large scale, similar to the population of mobile phone users, yet the bandwidth spectrum available for vehicular communications is very limited, great challenges are therefore brought to efficiently allocate the slim spectrum resource to vehicle users towards the best service quality. Therefore, it is of great importance to properly allocate spectrum resource to satisfy various safety related

1524-9050 © 2018 IEEE. Personal use is permitted, but republication/redistribution requires IEEE permission.
See http://www.ieee.org/publications_standards/publications/rights/index.html for more information.

Authorized licensed use limited to: XIDIAN UNIVERSITY. Downloaded on November 30,2020 at 06:31:03 UTC from IEEE Xplore. Restrictions apply.

and entertainment related applications for vehicles, and thus enhance traffic safety of intelligence transportation systems and improve the quality of experience of vehicular users. However, few literature studies the spectrum resource allocation in LTE-V networks, and majority of the existing works concerning vehicular networks have focused on the resource allocation without taking the diversity of vehicles and services into consideration. However, in practical scenario, vehicles with different types may request services with the same priority, or vehicles with the same type may request services with different priorities, for example, high priority vehicles (e.g, police cars or ambulances), public buses and private cars request real-time and safety-related services simultaneously, or several private cars request high priority services and infotainment services simultaneously. Therefore, it is critical to evaluate the *service importance* (SI) by jointly considering the priority of vehicle (PoV) and priority of service (PoS) and then allocate spectrum resource to those vehicles or services. Moreover, most of existing works just focus on spectrum allocation of cognitive radio instead of applying the cognitive radio technology to vehicular communications. Different from conventional resource allocation methods, available spectrum allocation methods mainly include game theory [13]–[15], auction mechanism [16]–[18] and graph coloring [19]–[21], which are generally applied to the scenarios with relatively static network topology and consume large computation.

In this work, we develop a two-dimensional priority table including PoV and PoS to evaluate the SI. Considering the interference between users, a graph coloring model is then utilized. As for the spectrum allocation, based on artificial immune system (AIS) that is a new intelligent method simulating natural immune system and has enormous potential to supply novel methods to solve complex resource allocation and optimization issues [22], we propose a novel immune clonal based spectrum allocation approach (IC-SRAA) to optimize the utility for the spectrum allocation.

The major contributions of this paper are four-fold.

- *Two-dimensional service importance evaluation*: we classify both vehicles and services into three types respectively and design a two-dimensional service importance evaluation method by comprehensively considering the vehicle priority and service priority, which, to the best of our knowledge, has rarely been investigated in previous literatures.
- *Graph coloring model*: in order to reuse the spectrum resource of cellular base station at maximum efficiency, we adopt the graph coloring model to avoid the interference between vehicles, where the process of spectrum resource allocation is the process of coloring the vehicles. Any two vertexes with a common edge cannot be colored as the same color, by which interference between two adjacent vehicles is avoided.
- *Immune clonal algorithm*: we formulate the spectrum resource allocation problem as a mixed integer programming (MIP) problem combined with the characteristic of stochastic program. By exploring the special structure of the formulated MIP and transforming the MIP gradually, we propose a novel immune clonal algorithm and the convergence of the proposed algorithm is proved.
- *Validation*: we conduct extensive simulations to verify our proposed algorithm. Simulation results validate the convergence and effectiveness of the algorithm and show that our proposed algorithm outperforms the typically genetic based spectrum resource allocation algorithm in terms of convergence and delay, which contributes to the improvement of safety in the road for ITS.

The rest of this paper is organized as follows. Section II reviews more related work. In Section III, we present the spectrum allocation problem and describe our system model and proposed service importance evaluation method, introduces the graph coloring model. And we propose an immune clonal based algorithm to solve the spectrum allocation issue in Section IV. Performance of our algorithm is evaluated in Section V and Section VI concludes the paper with closing remarks and presents the prospect of our future work.

II. Related Works

This section studies the related works on resource allocation, especially on spectrum resource allocation, and some state-of-the-art optimization algorithms to solve the resource allocation issue.

As for the resource allocation and optimization, W. Wu *et al.* [23] design an adaptive cross-layer resource allocation algorithm and employ a stochastic optimization model to maximize the network utility. And the problem of stochastic optimization of resource allocation is decomposed into two subproblems by the Lyapunov optimization theory, associated with the flow control in transport layer and the power allocation in physical (PHY) layer, respectively. For avoiding the signaling overhead, outdated dynamic information, and scalability issues, the distributed resource allocation method is developed for solving the two subproblems based on the primal-dual decomposition theory. Zhang *et al.* [24] investigate the resource scheduling for heterogeneous vehicular networks, where some moving vehicles are selected and scheduled as helping relays to assist information transmission between the roadside infrastructure and other moving vehicles. For such a system, a mobile-service based max-min fairness resource scheduling scheme is proposed, where service amount which is more suitable for high mobility scenarios is adopted to characterize the information transmission capacity of the links and the max-min criteria is adopted to meet the fairness requirement of the moving vehicles.

Considering the high mobility of users, Karimi *et al.* [25] present a novel LTE-based solution to support high throughput and continuous multimedia services for high speed train passengers. In order to accommodate the extreme channel variations, a scheduling and resource allocation mechanism is further proposed to maximize the service rate based on periodical signal quality changes. Liang and Zhuang [26] formulate an optimal resource allocation problem which is transformed into a single-machine preemptive scheduling problem with integer request times, processing times, and deadlines. As the service demands are not known a priori, an online resource

Authorized licensed use limited to: XIDIAN UNIVERSITY. Downloaded on November 30,2020 at 06:31:03 UTC from IEEE Xplore. Restrictions apply.

allocation algorithm based on Smith ratio and exponential capacity is proposed. If the link from the backbone network to an infostation is a bottleneck, a service pre-downloading algorithm is also proposed to facilitate the resource allocation.

Most of the existing resource allocation and optimization issues are integer linear programs (ILPs) and they are also NP-hard problems, which are not computable in polynomial time with existing general time with existing general solvers (e.g., MATLAB bintprog and brute-force method) [10]. Chen *et al.* transform the ILP into an equivalent binary linear program (BLP) in [10]. Wu *et al.* [23] propose a dynamic optimization method to decompose the optimization problem into two subproblems, and by solving the two subproblems respectively, the near-optimal solution is derived.

Other resource allocation methods such as game theory and graph coloring are also the research focuses. Wei *et al.* [27] propose a cloud resource allocation model based on an imperfect information Stackelberg game model (CSAM-IISG) to solve resource allocation in the cloud computing environment, where CSAM-IISG is used to determine the price, optimize the profit according to the current market situation quickly and flexibly, and achieve a Nash equilibrium. Kang *et al.* [28] investigate price-based resource allocation strategies for spectrum-sharing femtocell networks and then a Stackelberg game is formulated to study the joint utility maximization of the macrocell and femtocells.

As an intelligent method, graph coloring has became an important technique to solve the resource allocation problem, Bao *et al.* [29] propose an improved maximal weighted independent set-based graph coloring spectrum allocation algorithm that allocates spectrum to the nodes with maximal weighted independent set and fully considers the differences in spectral efficiency and interference spectral differences. Tan *et al.* [30] propose a graph theory based dynamic subband allocation technique to avoid downlink interference in a macrocell-femtocell overlay network. The cells and their mutual interference are modeled as graph elements, nodes and weighted edges, respectively. To maintain a tolerable interference level, the total bandwidth is divided into a number of sub-bands, and these are assigned to the femtocells using a graph coloring algorithm.

III. System Description

This section describes the considered system including the system model, the two-dimensioned service importance evaluation, the graph coloring model and the spectrum allocation problem formulation. For convenience, the main notations used throughout this paper are summarized in Table I.

A. System Model

We consider a LTE-V communication scenario where a cellular network supports on-demand data service delivery to moving vehicles. As shown in Fig. 1, different kinds of vehicles request on-demand data services through the cellular link. Suppose that the total spectrum resource $\mathcal{M}$ is divided into M spectrum resource blocks (SRBs), Let $\mathbb{M} = \{1, 2, 3, \cdots, M\}$ denote the set of SRBs and $\mathbb{N} = \{1, 2, 3, \cdots, N\}$ denote the set of N vehicles. The cellular network is assumed to be operated in slotted time, with time-slots normalized to integer values $t \in \mathbb{T} = \{0, 1, 2, \cdots, T\}$. Let $(x_n(t), y_n(t))$ be the position of vehicle n ($n \in \mathbb{N}$) at the beginning of time-slot t. For simplicity, the spectrum allocation is assumed to be operated at the beginning of each time-slot and remain unchanged during the current time-slot.

TABLE I

Major Notations

Notation	Definition
$\mathbb{M}$	The set of SRBs
$\mathbb{N}$	The set of vehicles
$\mathbb{T}$	The set of time-slots
$\mathcal{B}$	The total bandwidth
B_n	The allocated bandwidth resource for vehicle n
$u_{n,m}(t)$	Transmission rate between cellular base station and vehicle n at time-slot t
Ω_n	Received power of vehicle n
P_t	Transmission power of cellular base station
G_t	Transmission antenna gain
G_r	Reception antenna gain
h_t	Transmission antenna length
h_r	Reception antenna length
α	The path loss exponent
L	The loss coefficient of the system
N_0	The power spectral density of additive white Gaussian noise
p_n^1	The value of PoV
p_n^2	The value of PoS
$\mathbb{V}^1$	The set of emergency-related vehicles
$\mathbb{V}^2$	The set of public-related vehicles
$\mathbb{V}^3$	The set of private-related vehicles
$\mathbb{S}^1$	The set of real-time services related to traffic safety
$\mathbb{S}^2$	The set of real-time services related to non-traffic
$\mathbb{S}^3$	The set of non-real-time services
$p_{n,s}$	The value of *service importance* for vehicle n requesting service s
$r_{i,m}$	The interference range of vehicle i when using SRB m
$d_{i,j}(t)$	Distance between vehicle i and vehicle j at time-slot t
L	Leisure matrix
B	Benefit matrix
C	Constraint matrix
A	Allocation matrix
$l_{n,m}(t)$	The availability of SRB m to vehicle n at time-slot t
$b_{n,m}^s(t)$	The benefit vehicle n with request service s obtains at time-slot t when SRB m is allocated
$c_{n,k,m}(t)$	The interference indicator between vehicle n and vehicle k when using the SRB m simultaneously at time- slot t
$a_{n,m}(t)$	The allocation of SRB m to vehicle n at time-slot t
$U_{r_n}(t)$	The utility function of vehicle n at time-slot t
U_R	The overall benefit of the LTE-V communication

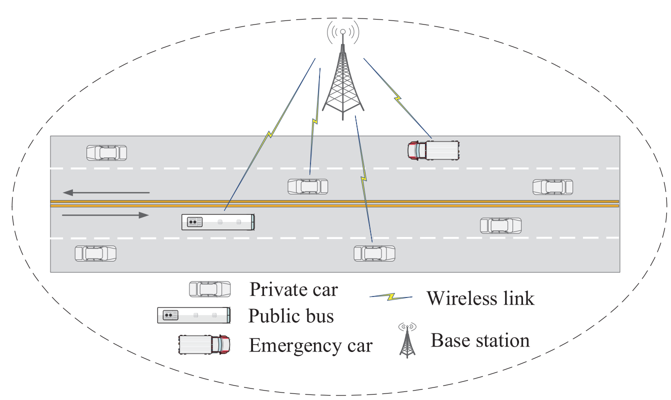

Fig. 1. System model.

Authorized licensed use limited to: XIDIAN UNIVERSITY. Downloaded on November 30,2020 at 06:31:03 UTC from IEEE Xplore. Restrictions apply.

Let $\mathcal{B}$ denote the total bandwidth corresponding to the spectrum resource $\mathcal{M}$, let B_m denote the allocated bandwidth resource for spectrum resource block m, and let the binary variable $a_{n,m}(t)$ indicate the allocation of SRB m to vehicle n at time-slot t, which is 1 when SRB m is allocated to vehicle n or 0 when it is not allocated to vehicle n. Without loss of generality, and under the framework of the Shannon formula, the theoretical transmission rate between cellular base station and vehicle n ($n \in \mathbb{N}$) at time-slot t is adopted and can be represented as

$$u_{n,m}(t) = a_{n,m}(t)B_n(t)\log_2(1 + \frac{\Omega_n}{B_n(t)N_0}), \tag{1}$$

where N_0 is the power spectral density of additive white Gaussian noise, and Ω_n is the received power of vehicle n, which is defined as

$$\Omega_n = P_t G_t G_r \frac{h_t^2 h_r^2}{d_n^{\alpha} L}, \tag{2}$$

where P_t is the transmission power of cellular base station, G_t and G_r are the transmission and reception antenna gains respectively, h_t and h_r are the transmission and reception antenna length respectively, L is the loss coefficient of the system, d_n denotes the distance between cellular base station and vehicle n, and α represents the path loss exponent.

B. Two-Dimensional Service Importance Evaluation

Since vehicles with different types may request different services and the limited spectrum resource should be first allocated to vehicles or services with high priority, SI should be evaluated first by jointly considering the classes of vehicles and services. In this paper, services and vehicles are both classified into three classes as a function of their attributes. Let $\mathbb{V}^1$, $\mathbb{V}^2$ and $\mathbb{V}^3$ ($\mathbb{V}^1 \cup \mathbb{V}^2 \cup \mathbb{V}^3 = \mathbb{N}$) denote the sets of emergency-related vehicles (e.g., ambulance, police car and fire truck), public-related vehicles (e.g., bus) and private-related vehicles (e.g. car and truck), respectively. Let $\mathbb{S}^1$, $\mathbb{S}^2$ and $\mathbb{S}^3$ denote the sets of real-time services related to traffic safety, real-time services related to non-safety and non-real-time services, respectively. For each vehicle n ($n \in \mathbb{N}$) and request service s ($s \in \mathbb{S}^1 \cup \mathbb{S}^2 \cup \mathbb{S}^3$), their priorities are formulated as

$$p_n^1 = \begin{cases} 1, \ n \in \mathbb{V}^1, \\ 2, \ n \in \mathbb{V}^2, \\ 3, \ n \in \mathbb{V}^3. \end{cases} \tag{3}$$

$$p_s^2 = \begin{cases} 1, \ s \in \mathbb{S}^1, \\ 2, \ s \in \mathbb{S}^2, \\ 3, \ s \in \mathbb{S}^3. \end{cases} \tag{4}$$

where p_n^1 and p_s^2 represent the values of PoV and PoS, respectively, 1 indicates the highest priority, 3 indicates the lowest. Due to the diversity of services and vehicles, it is necessary to evaluate the *service importance* by jointly considering PoV and PoS. We assume that the priority of vehicle is more important than that of service. And three rules for comprehensively evaluating *service importance* are adopted: 1) the higher the PoV, the greater the SI, 2) the SI of the real-time services related to traffic safety is higher; 3) with the same PoV, the higher PoS, the greater the SI. Accordingly, we reference the priority table based real-time scheduling method used in operation system, the evaluation of SI $p_{n,s}$ is formulated as

TABLE II

TWO-DIMENTIONAL SI EVALUATION-I

SI \ *PoS* / *PoV*	1	2	3
1	1	2	4
2	3	5	**8**
3	6	**9**	**13**

TABLE III

TWO-DIMENTIONAL SI EVALUATION-II

SI \ *PoS* / *PoV*	1	2	3
1	1	4	5
2	2	6	**7**
3	3	**8**	**9**

$$p_{n,s} = (\gamma\,(p_n^1 - 1 - \mu) + 2p_s^2 - 2)\frac{p_n^1 + \mu}{2} + p_n^1, \tag{5}$$

$$\mu = \left\lfloor \frac{p_s^2 - 2}{\gamma} \right\rfloor, \tag{6}$$

where γ is a weighing factor reflecting the preference to the PoV, $\lfloor \cdot \rfloor$ denotes the floor function, p_n^1 and p_s^2 represent the values of PoV and PoS, derived from Eq. 3 and Eq. 4, respectively. In this paper, we set $\gamma = 1$, then the representation of *service importance* $p_{n,s}$ is formulated as

$$p_{n,s} = (p_n^1 + p_s^2 - 1)\frac{p_n^1 + p_s^2 - 2}{2} + p_n^1. \tag{7}$$

According to Eq. 7, a two-dimensional SI table can be easily obtained as shown in Table II, now we adjust the table according to the rule that SI of the real-time services related to traffic safety is higher, and note that SI has 9 levels, i.e., $p_{n,s} \in \{1, 2, 3, 4, 5, 6, 8, 9, 13\}$, 1 indicates the most important SI. For simplicity, we let the value of 8, 9 and 13 be replaced by 7, 8 and 9, respectively, which is presented in Table III.

C. Graph Coloring Model

After the evaluation of SI, spectrum resource should be first allocated to the vehicles with smaller SI value and optimized spectrum resource allocation algorithm should be performed at the same time so that the LTE-V system benefits most. In order to improve the spectral efficiency, vehicles must reuse the spectrum resource, which will induce interference between vehicles. In this paper, a graph coloring model is proposed to avoid interference, as illustrated in Fig. 2. We assume that all vehicles are equipped with cognitive radios that are enabled to implement various functionalities, including frequency agility, transmit power control and access coordination, which render more efficient use of available spectrum [31]. The self-interference, experienced at the cellular base station or a

Authorized licensed use limited to: XIDIAN UNIVERSITY. Downloaded on November 30,2020 at 06:31:03 UTC from IEEE Xplore. Restrictions apply.

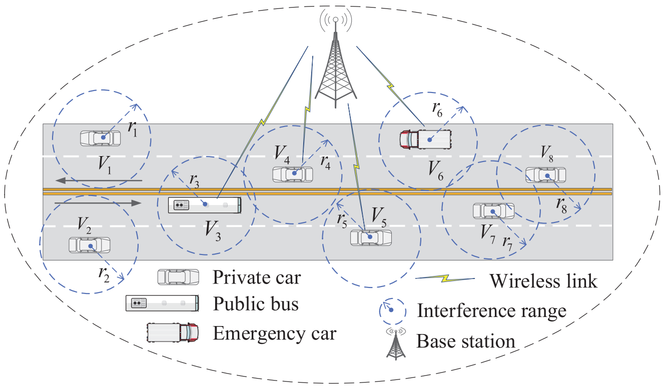

Fig. 2. Graph coloring model.

vehicle resulting from their transmission to their reception over the same SRB, can be sufficiently suppressed by using existing self-interference cancellation methods, such as the distributed linear convolutional space-time coding (DLC-STC) [32], [33]. Let $r_{n,m}$ $(n \in \mathbb{N}, m \in \mathbb{M})$ denote the interference range of vehicle n when using SRB m, which means that if two vehicles (i and j) use the same spectrum resource, vehicle i will induce interference to vehicle j only when

$$r_{i,m} + r_{j,m} > d_{i,j}(t), \tag{8}$$

where $d_{i,j}(t) = \sqrt{(x_i(t) - x_j(t))^2 + (y_i(t) - y_j(t))^2}$ is the distance between vehicle i and vehicle j at time-slot t. We assume that no co-channel interference exists if two vehicles satisfy Eq. 8.

We model the spectrum resource allocation as graph coloring, where the process of spectrum resource allocation is the process of coloring the vehicles. We represent the sensed network topology as an undirected conflict graph $G = (V, S, E)$, where $V = \{v_n | n = 1, 2, 3, \cdots, N\}$ is vertex set, with each vertex representing a vehicle; S denotes the color list representing the color of each vertex, i.e., available spectrum resource; $E = \{e_{ij} | i, j = 1, 2, 3, \cdots, N\}$ is the undirected edge set, where $e_{ij} = 0$ represents the disconnection between vehicle i and vehicle j and they can use the same spectrum resource, $e_{ij} = 1$ represents the connection between vehicle i and vehicle j and they cannot use the same spectrum resource. Therefore, the coloring condition corresponding to available spectrum resource allocation can be described as: when two vertexes have a common edge colored as m (i.e., spectrum resource m), the two vertexes cannot be colored as m simultaneously (i.e., two vehicles cannot use the same spectrum resource m).

D. Problem Formulation

Since different vehicles can obtain different spectrum resource, we consider a SI-and-rate based utility function for the LTE-V communication. The purpose of the spectrum allocation is to maximize the utility of the whole network. According to the graph coloring model, spectrum resource allocation can be modeled as the following matrixes: Leisure Matrix (L), Benefit Matrix (B), Constraint Matrix (C) and Allocation Matrix (A). The definitions of those matrixes are as follows.

Definition 1: Leisure Matrix (L) is defined as the available spectrum resource not occupied by any vehicle, whether a SRB is available to a vehicle at time-slot t can be represented by $L(t)$, and is denoted as

$$L(t) = \{l_{n,m}(t) | l_{n,m}(t) \in \{0, 1\}\}_{N \times M}, \tag{9}$$

where $l_{n,m}(t)$ indicates the availability of SRB m to vehicle n, which is 1 when m is available to n or 0 when m is not available to n.

Definition 2: Benefit Matrix (B) is the benefit vehicle gets, denoted as

$$B(t) = \{b^s_{n,m}(t) | n \in \mathbb{N}, m \in \mathbb{M}, s \in \mathbb{S}^1 \cup \mathbb{S}^2 \cup \mathbb{S}^3\}_{N \times M}, \tag{10}$$

where $b^s_{n,m}(t)$ denotes the benefit vehicle n with request service s obtains at time-slot t when SRB m is allocated to it. In this paper, the benefit is represented by the SI-and-rate based utility function, which is defined as

$$\begin{aligned} b^s_{n,m}(t) &= \frac{1}{p_{n,s}} \ln(u_{n,m}(t)) \\ &= \frac{2(a_{n,m}(t) B_n(t) log_2(1 + \frac{\Omega_n}{B_n(t) N_0}))}{(p^1_n + p^2_s - 1)(p^1_n + p^2_s - 2) + 2 p^1_n}, \end{aligned} \tag{11}$$

where Ω_n denotes the received power of vehicle, which is defined as Eq. 2. It is obvious that $b^s_{n,m}(t)$ equals 0 when $l_{n,m}$ equals 0.

Definition 3: Constraint Matrix (C), also named interference matrix, indicates the interference between vehicles, which is denoted as

$$\begin{aligned} C(t) = \{&c_{n,k,m}(t) | c_{n,k,m}(t) \in \{0, 1\}, n, k \in \mathbb{N}, \\ &m \in \mathbb{M}\}_{N \times N \times M}, \end{aligned} \tag{12}$$

where $c_{n,k,m}(t)$ indicates the interference between vehicle n and vehicle k when using the SRB m simultaneously at time-slot t, which is 1 when interference exits or 0 when no interference exits. $C(t)$ is determined by available spectrum resource and distance between vehicles. It is noted that when $n = k$, we have $c_{n,n,m}(t) = 1 - l_{n,m}(t)$, and interference exits only when SRB m is available to vehicle n and vehicle k simultaneously at time-slot t. Accordingly, from Eq. 8, we have

$$c_{n,k,m}(t) = \begin{cases} 0, & r_{n,m} + r_{k,m} \le d_{n,k}(t), n \ne m, \\ 1, & r_{n,m} + r_{k,m} > d_{n,k}(t), n \ne m, \\ 1 - l_{n,m}(t), & n = m. \end{cases} \tag{13}$$

$$s.t. \quad c_{n,k,m}(t) \le l_{n,m}(t) + l_{k,m}(t). \tag{14}$$

Definition 4: Allocation Matrix (A) is the available spectrum resource allocated to vehicles with no interference, and is denoted as

$$A(t) = \{a_{n,m}(t) | a_{n,m}(t) \in \{0, 1\}, n \in \mathbb{N}, m \in \mathbb{M}\}_{N \times M}, \tag{15}$$

where $a_{n,m}(t)$ denotes the allocation of SRB m to vehicle n at time-slot t, which is 1 when SRB m is allocated to vehicle n or 0 when it is not allocated to vehicle n. And A must meet the no interference constrain defined by C as

$$a_{n,m}(t) a_{k,m}(t) = 0, \;\; c_{n,k,m}(t) = 1, \;\; \forall n, k \in \mathbb{N}, \forall m \in \mathbb{M}. \tag{16}$$

Authorized licensed use limited to: XIDIAN UNIVERSITY. Downloaded on November 30,2020 at 06:31:03 UTC from IEEE Xplore. Restrictions apply.

According to the definition and analysis above, there exits not only one Allocation Matrix A that meet the constrains. For a certain A, the profit brought by the allocation for vehicle n requesting service s at time-slot t can be characterized by the utility of SI and transmission rate, which is given by

$$U_{r_n}(t) = \sum_{m=1}^{M} a_{n,m}(t) b_{n,m}^{s}(t), \tag{17}$$

then the overall benefit of the LTE-V communication is characterized by

$$U_R(t) = \sum_{n=1}^{N}\sum_{m=1}^{M} a_{n,m}(t) b_{n,m}^{s}(t), \tag{18}$$

where R is the vector of the SI-and-rate based utility for all vehicles. To maximize the average SI-and-rate based utility of the LTE-V communication, the spectrum resource allocation and optimization problem can be formulated as

$$\begin{aligned}
(\mathbf{P1}) \quad \max \quad & U_{\boldsymbol{R}} = \frac{1}{T}\sum_{t=0}^{T}\sum_{n=1}^{N}\sum_{m=1}^{M} a_{n,m}(t) b_{n,m}^{s}(t) \\
s.t.\ \text{1-C1}: & \sum_{n=1}^{N}\sum_{m=1}^{M} a_{n,m}(t) B_n(t) \leq B, \quad \forall t \in \mathbb{T} \\
\text{1-C2}: & c_{n,k,m}(t) \in \{0,1\}, \quad \forall n,\ k \in \mathbb{N}, m \in \mathbb{M} \\
\text{1-C3}: & A(t) = \{a_{n,m}(t) | a_{n,m}(t) \in \{0,1\}, \\
& n \in \mathbb{N}, \quad m \in \mathbb{M}\}_{N\times M},
\end{aligned} \tag{19}$$

where the detailed expression and constrains of 1-C2 are formulated as Eq. 13 and Eq. 14.

In the formulated optimization problem P1, B denotes the maximum bandwidth corresponding to the spectrum resource. 1-C2 describes the interference between vehicles from the perspectives of position and spectrum resource. 1-C3 ensures that no interference will be brought under the condition that two vehicles use the same SRB simultaneously and interference exits from the perspective of position. 1-C2 and 1-C3 jointly ensure that SRBs can be allocated to vehicles with no interference.

Problem P1 is a mixed integer programming (MIP) problem combined with the characteristic of stochastic program, which cannot be solved efficiently [3], [26]. For simplicity, we assume the spectrum resource allocation is independent in each time-slot, so the spectrum resource allocation is only considered in one time-slot. Therefore, problem P1 can be reformulated as

$$\begin{aligned}
(\mathbf{P2}) \quad \max \ & U_{\boldsymbol{R}} = \sum_{n=1}^{N}\sum_{m=1}^{M} a_{n,m} b_{n,m}^{s} \\
s.t.\ \text{2-C1}: & \sum_{n=1}^{N}\sum_{m=1}^{M} a_{n,m} B_n \leq B \\
\text{2-C2}: & c_{n,k,m} \in \{0,1\}, \quad \forall n,\ k \in \mathbb{N},\ m \in \mathbb{M} \\
\text{2-C3}: & A = \{a_{n,m} | a_{n,m} \in \{0,1\}, \\
& n \in \mathbb{N}, \quad m \in \mathbb{M}\}_{N\times M},
\end{aligned} \tag{20}$$

where 2-C1, 2-C2 and 2-C3 are converted from 1-C1, 1-C2 and 1-C3 in Eq. 19 excluding the time-slot variable t, respectively.

IV. Proposed Spectrum Resource Allocation Algorithm

It is impossible to solve the optimization problem P2 in polynomial time, because it is modeled as a MIP problem, which has been shown to be NP-hard [3], [34]. In order to solve P2, we first divide the continuous bandwidth resource into discrete bandwidth resource blocks (BRBs), with each BRB mapping to a SRB. Then we propose an immune clonal based intelligent algorithm to solve the spectrum resource allocation problem. What follows, we will present our proposed scheme in detail.

A. Bandwidth Resource Mapping

In order to reduce the complexity of the problem P2, in our work, we divide the continuous bandwidth resource into M discrete BRBs, with each size of $\mathcal{B}/M$ and each BRB mapping to a SRB. Therefore, the allocation of bandwidth resource comes down to the allocation of spectrum resource. Then problem P2 can be reformulated as

$$\begin{aligned}
(\mathbf{P3}) \quad \max \ & U_{\boldsymbol{R}} = \sum_{n=1}^{N}\sum_{m=1}^{M} a_{n,m} b_{n,m}^{s} \\
s.t.\ \text{3-C1}: & c_{n,k,m} \in \{0,1\}, \quad \forall n,\ k \in \mathbb{N},\ m \in \mathbb{M} \\
\text{3-C2}: & A = \{a_{n,m} | a_{n,m} \in \{0,1\}, \\
& n \in \mathbb{N}, \quad m \in \mathbb{M}\}_{N\times M},
\end{aligned} \tag{21}$$

where 3-C1 and 3-C2 are the same as 2-C2 and 2-C3 in Eq. 20, respectively.

B. Artificial Immune System

The spectrum allocation problem P3 can be described as: given the L, B and C, how to find the optimal A for maximizing U_R. Motivated by the artificial immune system (AIS), we propose an immune clonal algorithm to solve the spectrum allocation problem P3 in this paper. AIS is a new intelligent optimization method simulating natural immune system, and it has the ability to solve complex problems and is becoming another research hot point in the artificial intelligent techniques after neural network, fuzzy system, and evolutionary computation [22]. In order to describe the algorithm explicitly, we define the terms as follows.

1) *Antigen*: In immunology, an antigen is any substance that causes the immune system to produce antibodies against it. In this paper, the antigen is defined as the objective function U_R.

2) *Antibody*: In immunology, B cells, T cells, and antigen-specific lymphocytes are generally called antibodies. In this paper, an antibody is a representation of a candidate solution of P3.

3) *Antibody Population*: A antibody population consists of several antibodies, and the number of antibodies a population consists of is the scale of the population.

4) *Fitness*: Fitness value is the value of the objective function. Each antibody has a fitness value, which represents whether the antibody is suitable to be the final solution. The higher the fitness value, the more suitable is the antibody as the final solution. In this paper, the fitness value is the utility function of the LTE-V communication, i.e., the value of U_R.

Authorized licensed use limited to: XIDIAN UNIVERSITY. Downloaded on November 30,2020 at 06:31:03 UTC from IEEE Xplore. Restrictions apply.

5) *Population Coding*: How to use the antibody to represent the resource allocation result and how to acquire the resource allocation result from an antibody are very important. In this paper, binary coding is used to represent the elements in A.

6) *Fitness Evaluation*: Calculate the fitness value (i.e., the value of objective function U_R) for each antibody.

7) *Clone Operation*: Create more of the same antibodies using one antibody. In this paper, it means creating more of the same A.

8) *Mutation Operation*: Change the value of some genes of an antibody, which adjusts the resource allocation result in a small extent. In this paper, it means changing the value of a randomly picked element in A.

9) *Population Updating*: Use antibodies with high fitness values to replace antibodies with low fitness values.

C. Immune Clonal Based Spectrum Resource Allocation

In this section, we describe the proposed immune clonal based spectrum resource allocation algorithm which is similar to the genetic algorithm [35]. In the algorithm, the initialization, modification of A, population coding, fitness evaluation, judgement of termination condition, clone operation, mutation operation, and population updating operation are described as follows.

1) Initialization: Initialize the iterative number g:=0, generate the initial population $\boldsymbol{P}(g)$ randomly as

$$\boldsymbol{P}(g) = \{P_1(g), P_2(g), ..., P_{s'}(g)\}, \tag{22}$$

where s' denotes the size of the population. A memory unit $MU(g)$ with the size of t' is set and initialized void. Binary encoding is adopted for each antibody. The length of each antibody is formulated as

$$l = \sum_{n=1}^{N}\sum_{m=1}^{M} l_{n,m}, \tag{23}$$

namely, l represents the number of none-zero elements in L. And each antibody represents a possible allocation scheme. At the same time, record n and m that meet $l_{n,m} = 1$ in L respectively. Then store them in L_1 in the form of n increasing first, m increasing later. Namely, $L_1 = \{(n, m)|l_{n,m} = 1\}$, obviously, there are l elements in L_1.

2) Mapping of Antibody Representation to Spectrum Allocation Scheme: Map each bit j $(1 \le j \le l)$ of each antibody $P_i(g)$ $(1 < i < s')$ in the antibody population to the element $a_{n,m}$ in A, where the value of (n, m) is the j^{th} element j $(1 \le j \le l)$ in L_1. Then, the corresponding A is a possible allocation scheme.

*3) Modification of **A**:* The interference matrix C must be taken into consideration for the allocation solution. Based on C, we first need to modify L. The process of the modification is described as: for arbitrary m, if $c_{n,k,m} = 1$, then check whether the two elements $l_{n,m}$ and $l_{k,m}$ are both equal to 1. If so, set one of the two elements as 0, with another unchanged. After the interference handling, the modified L becomes the feasible solution A. At the same time, map the corresponding antibody representation and update $\boldsymbol{P}(g)$.

4) Fitness Evaluation: Since the purpose of spectrum allocation is to maximum the utility of the LTE-V communication, we regard U_R as the fitness function. We first calculate the fitness of each antibody in $\boldsymbol{P}(g)$ and sort the results in descending order, then update $MU(g)$ with t $(t' < s')$ high-fitness antibodies (if $MU(g)$ is empty, store the t' antibodies in $MU(g)$ directly; otherwise, conduct replacement according to the values of fitness, ensuring that the t' antibodies with the most high fitness are remained). Accordingly, the allocation solution A corresponding to the antibody with the most high fitness in $MU(g)$ is the optimal spectrum allocation solution.

5) Judgement of Termination Condition: If reach the termination generation $g_{\max}$, map the antibody with the most high fitness value in $MU(g)$ to the form of A, i.e., the optimal spectrum allocation is obtained; Otherwise, go to step *6)*.

6) Clone Operation: The clone operation T_{c}^{C} on the antibody population $\boldsymbol{P}(g)$ is defined as

$$\boldsymbol{P}'(g) = T_{\mathrm{c}}^{C}(\boldsymbol{P}(g)) = [T_{\mathrm{c}}^{C}(P_1(g)), \cdots, T_{\mathrm{c}}^{C}(P_{t'}(g))]^T. \tag{24}$$

The specific clone operation is described as follows. Assuming the selected t' antibodies are sorted in descending order as $P_1(g), P_2(g), \cdots, P_{t'}(g)$, then the number of antibodies cloned from the qth antibody $P_q(g)$ $(1 \le q \le t')$ is formulated as

$$N_q = Int(\frac{n_t f(P_q(g))}{c_{(P_q(g))} \sum_{h=1}^{t'} f(P_h(g))}), \tag{25}$$

where $Int(a)$ denotes the ceil function (the smallest integer greater than or equal to a), $f(\cdot)$ denotes antibody fitness, $n_t > t'$ is a control parameter, $c_{(P_q(g))}$ denotes the antibody concentration of antibody $P_q(g)$, which is formulated as

$$c_{(P_q(g))} = \sum_{h=1}^{t'} S(P_q(g), P_h(g)), \tag{26}$$

where $S(\cdot)$ denotes the set of the similar antibodies, which is defined as

$$S(P_q(g), P_h(g)) = \begin{cases} 1, \ d(P_q(g), P_h(g)) < \theta, \\ 0, \ otherwise. \end{cases} \tag{27}$$

where $d(\cdot)$ denotes the Hamming distance, θ is a threshold.

The above equations show that the greater fitness value of antibody and the less antibody concentration, the larger the clone scale.

After the clone operation, the population is denoted as

$$\boldsymbol{P}'(g) = \{(P'_1(g)), (P'_2(g)), \cdots, (P'_{t'}(g))\}. \tag{28}$$

7) Mutation Operation: The mutation operation on the population after cloning $\boldsymbol{P}'(g)$ with the probability of p_m can be described as

$$p(P'_i(g) \to P''_i(g)) = (p_m)^{d(P'_i(g), P''_i(g))}(1 - p_m)^{(l - d(P'_i(g), P''_i(g)))} \tag{29}$$

where l denotes the coding length of antibody. As far as the binary representation is concerned, mutation operation makes some elements inverse with the probability of p_m (i.e., $1 \to 0$ or $0 \to 1$).

Authorized licensed use limited to: XIDIAN UNIVERSITY. Downloaded on November 30,2020 at 06:31:03 UTC from IEEE Xplore. Restrictions apply.

After the mutation operation, the population is denoted as

$$\boldsymbol{P}''(g) = \{(P''_1(g)), (P''_2(g)), \cdots, (P''_{t'}(g))\}. \tag{30}$$

8) Population Updating Operation: In order to maintain the stability of population scale s', if $\sum_{q=1}^{t'} N_q < s'$, randomly generate $s' - \sum_{q=1}^{t'} N_q$ new antibodies for supplement; otherwise, select the first s' antibodies to form a new antibody population, which is denoted as $\boldsymbol{P}(g+1) = T_u^C(\boldsymbol{P}''(g))$. Then go back into step *2)*.

Proposition 1 (Convergency): The proposed algorithm converges with probability 1. Let B^* denote the global optimal solution, $\vartheta(\mathbf{P})$ denote the number of optimal solutions contained in population $\mathbf{P}$, then for arbitrary initial state $\mathbf{P}_0$, the following equation holds

$$\lim_{g\to\infty} p\{\boldsymbol{P}(g) \cap B^* \neq \varnothing | \boldsymbol{P}(0) = \boldsymbol{P}_0\} = \lim_{g\to\infty} p\{\vartheta(\boldsymbol{P}(g)) \geq 1 | \boldsymbol{P}(0) = \boldsymbol{P}_0\} = 1. \tag{31}$$

Proof: Please refer to appendix. □

V. Simulation and Numerical Results

In this section, we present some simulation results to discuss the system performance of our proposed IC-SRAA with respect to iterations, number of vehicles, ratio of SRBs to the number of vehicles, size of population and convergence. For comparison, we also simulate the genetic based spectrum resource allocation algorithm (G-SRAA) as benchmark scheme. We first outline the simulation setup. Then, we give and discuss the simulation results.

A. Simulation Scenario and Parameter Configurations

We simulate the LTE-V communication scenarios as shown in Fig. 1, where N vehicles are within the coverage area of one cellular base station. We assume that the total spectrum resource reserved for LTE-V communications is $\mathcal{B}$. In order to better evaluate the impact of various parameters on the system performance, we define φ as the ratio of the number of SRBs M to the number of vehicles N. The vehicles are initially randomly positioned on the road, and the values of PoV and PoS of each vehicle are randomly generated from the set $\{1, 2, 3\}$. Since we have converted the problem P1 to problem P3 that can be solved in any time-slot, for simplicity, we just simulate the performance in one time-slot. The detailed parameter settings are listed in Table IV.

TABLE IV
SIMULATION PARAMETERS

Parameter	Value
Length of per lane (m)	4000
Number of lanes	2
Width of per lane (m)	4
Number of vehicles N	$\{30, 40, 50\}$
Ratio of SRBs to the number of vehicles φ	{1,2,3,4,5,6}
Interference range of each vehicle (m)	125
Transmit power P_t (dBm)	43
Noise spectral density N_0 (dBm/Hz)	−174
Path loss index α	4
G_t, G_r, h_t, h_r, L	1
Termination generation $g_{\max}$	1500
Size of the population s'	{20,30,40,50}
Size of the memory unit t'	$\{10, 15, 20, 25\}$
Control parameter n_t	$\{20, 25, 30, 35\}$
Mutation probability p_m	0.3
Crossover probability p_c	0.3
Bandwidth resource $\mathcal{B}$ (MHz)	10

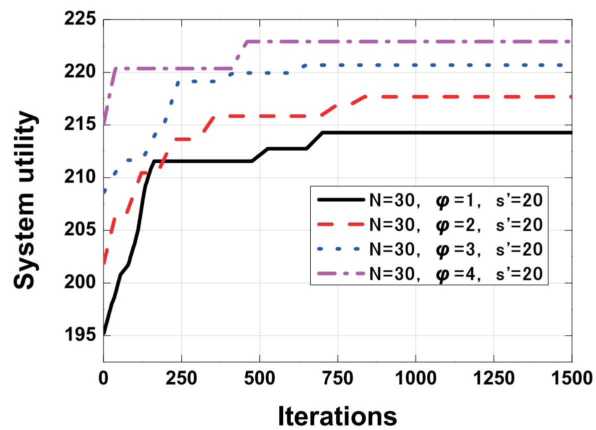

Fig. 3. System utility under different φ.

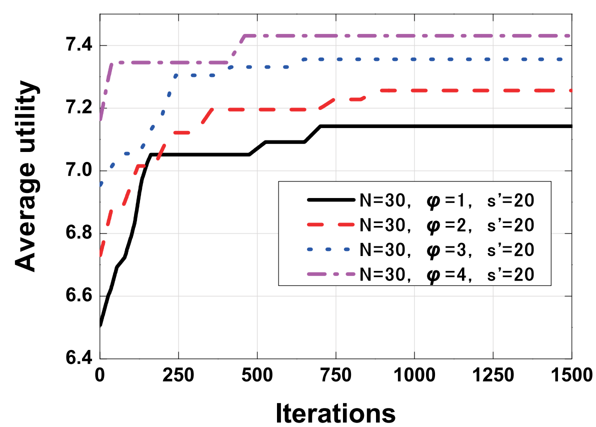

Fig. 4. Average utility under different φ.

B. SI-and-Rate Based Utility of the LTE-V Communication

We first compare the performance of system utility and average utility under different number of vehicles, SRBs (i.e., different φ) and population size, as shown in Fig. 3, Fig. 4, Fig. 5 and Fig. 6. In Fig. 3 and Fig. 4, we give the results for system utility and average utility varying with φ from 1 to 4 and iteration from 0 to 1500 when we fix $N = 30$ and $s' = 20$. The results for $\varphi = 1$, $\varphi = 2$, $\varphi = 3$ and $\varphi = 4$ are described by the black (solid), red (dash), blue (dot) and magenta (dash dot) lines respectively. Both the figures indicate that the system utility and average utility increase with the increase of iterations. And at the beginning of the iterations, the utilities increase rapidly. The season is that the proposed IC-SRAA algorithm performs the mutation operation and generates optimal population for the allocation scheme. Fig. 3 depicts the system utility varying with φ and iterations. Larger φ means higher system utility, and it

Authorized licensed use limited to: XIDIAN UNIVERSITY. Downloaded on November 30,2020 at 06:31:03 UTC from IEEE Xplore. Restrictions apply.

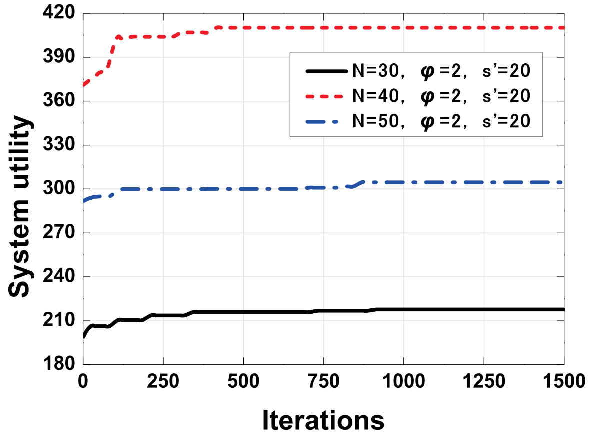

Fig. 5. System utility for different values of N over iterations.

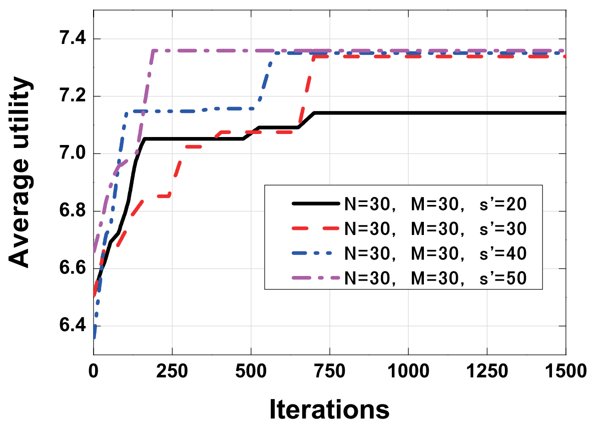

Fig. 6. The impact of s' on average utility and convergence speed.

means that if we divide the total spectrum resource to more resource blocks, more utilities the system can achieve. The reason is that once the total spectrum resource is fixed, more resource blocks means that the size of each resource block is very small and the discrete variable $\mathcal{B}/M$ in problem P3 can be equivalent to the continuous variable B_n in problem P1, which means that the optimal solution for problem P3 is more closer to the optimal solution in problem P1. Fig. 4 depicts the average utility varying with φ and iterations. Since the average utility is the ration of system utility to the number of vehicles, the variation tendency of four curves is the same as that in Fig. 3.

Let $s' = 20$ and $\varphi = 2$. Then, we reveal the variation of the system utility for different number of vehicles over iterations in Fig. 5. The results for $N = 30$, $N = 40$ and $N = 50$ are described by the black (solid), red (short dash) and blue (dash dot) lines respectively. Overall, the system utility of the three curves all converge to their respective stable values. Moreover, among the three values of the number of vehicles, $N = 40$ has the highest system utility and $N = 30$ has the lowest system utility, while the system utility of $N = 50$ between them, which means that the impact of the number of vehicles on average system is irregular. The reason is that, although more vehicles can lead to the increase of system utility, the probability that interference is caused between two adjacent vehicles also increases, especially when

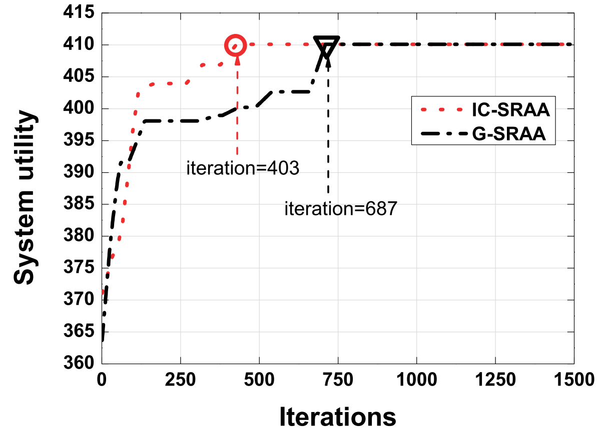

Fig. 7. The convergence of proposed IC-SRAA compared with G-SRAA.

the number of vehicles exceeds a certain threshold, resulting in that two or more adjacent vehicles cannot reuse the same bandwidth resource blocks.

Let $N = 30$ and $M = 30$ (i.e., φ=1). Then we reveal how the variation of population size s' affects the average utility. As shown in Fig. 6, the results for $s' = 20$, $s' = 30$, $s' = 40$ and $s' = 50$ are described by the black (solid), red (dash), blue (dash dot dot) and magenta (dash dot) lines respectively. The results from Fig. 6 indicate that the population size has a significant affect on the convergence speed, i.e., the larger the population size, the faster the convergence. The reason why the increase of s' can accelerate the convergence is that larger scale of population can maintain the diversity of antibodies thus increasing the opportunity that antibodies evolute to optimal antibodies. Furthermore, it is clear that the average utility increases as s' increases, and when s' increases to 30, 40 and 50, the optimal average utilities are almost the same, which guides us that in order to reduce computational complexity, for the given scale of the optimal problem, choosing $s' = 30$ is enough to obtain the optimal solution.

C. Convergence of the Proposed Solution

Through evaluating the system utility, Fig. 7 shows the convergence iterations for the proposed IC-SRAA compared with the genetic based spectrum resource allocation algorithm (G-SRAA). We fix $N = 40$, $\varphi = 2$ and $s' = 50$. The results for IC-SRAA and G-SRAA are described by the red (dot) and black (dash dot) lines respectively. It can be generally observed that the system utility of the proposed IC-SRAA converges to the optimal value about 410 after iteration=403 while the system utility of G-SRAA converges to the optimal value after interation=687. This is because that the memory unit (MU) is utilized to store t' antibodies with the highest fitness value in our proposed IC-SRAA, which is conductive to the rapid convergence of the proposed algorithm. Furthermore, there is no crossover operation after the mutation operation in IC-SRAA compared with the G-SRAA, which also accelerates convergence. In addition, in the process of clone operation, we adopt an adaptive clone method, where the antibody with high fitness value and low concentration has a larger clone scale. This adaptive clone method guarantees the diversity of

Authorized licensed use limited to: XIDIAN UNIVERSITY. Downloaded on November 30,2020 at 06:31:03 UTC from IEEE Xplore. Restrictions apply.

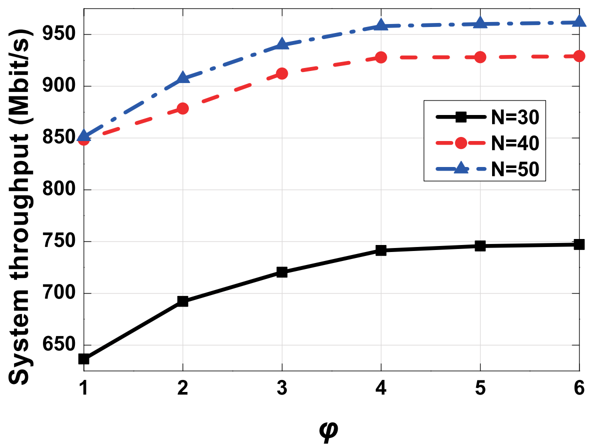

Fig. 8. System throughput under different N and φ.

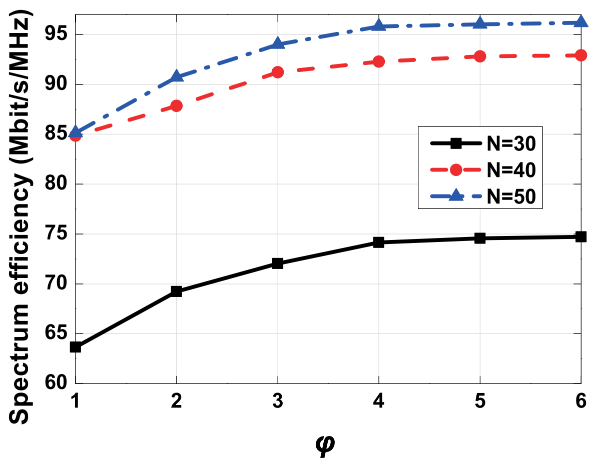

Fig. 9. Average throughput under different N and φ.

antibody population and avoids premature convergence which will result in a local optimum.

D. Throughput and Spectrum Efficiency

In the third simulation set, we aim at demonstrating the system throughput and spectrum efficiency of our proposal when the optimal solution has been achieved and we fix $s' = 50$. Thus, we plot as in Fig. 8 and Fig. 9, the system throughput and spectrum efficiency against φ for variable number of vehicles. The simulation results in Fig. 8 show that the system throughput for variable number of vehicles ($N = 30$, $N = 40$ and $N = 50$) are improved as φ increases in the beginning and maintain stable when φ reaches 5 and 6. The reason is that as φ increases, the SI-and-rate based utility of the LTE-V communication increases and obtains the optimal solution as explained in subsection V-B for Fig. 3 and Fig. 4. Hence, the system throughput increases correspondingly and maintains stable as the system utility stay stable. Furthermore, Fig. 8 plots the system throughput versus different number of vehicles, which shows that the system throughput increases as N increases. The reason is that our proposed algorithm reuses the available spectrum resource as long as no interference exits between two vehicles. More vehicles means that the

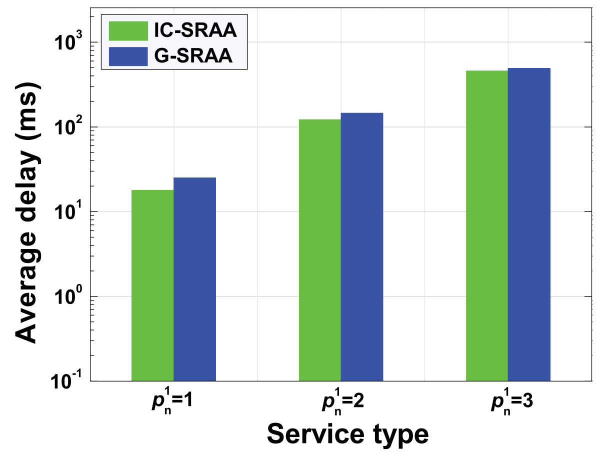

Fig. 10. Average delay for three different service types.

spectrum resource can serve more services thus resulting in the increase of system throughput. Obviously, the increase of the number of vehicles can prolong the system throughput. Since the spectrum efficiency characterizes the throughput that can be achieved over a given bandwidth, and the total bandwidth is fixed in our simulation of 10 MHz, the variation tendency of spectrum efficiency as shown in Fig. 9 is as the same as that of system throughput as shown in Fig. 8.

E. Average Delay

In the fourth simulation set, we aim at revealing the average delay for three different service types. We set $s' = 20$, $\varphi = 2$ and $N = 40$. Fig. 10 shows the average delay of the proposed IC-SRAA compared with G-SRAA for three different service types. The results for IC-SRAA and G-SRAA are described by green and blue bar graph respectively. For the horizontal axis of Fig. 10, $p_n^1 = 1$ represents the real-time services related to traffic safety, $p_n^1 = 2$ represents the real-time services related to non-safety, $p_n^1 = 3$ represents the non-real-time services. It can be generally observed that the average delay of both IC-SRAA and G-SRAA for $p_n^1 = 1$ is around 10 ms, while the magnitude of average delay for $p_n^1 = 3$ is in hundreds of milliseconds. This is due to the fact that the services with higher priority or vehicles with higher priority would be allocated to more SRBs for the purpose of obtaining the maximal utility in our formulated optimization problem. The real-time services related to traffic safety experience less delay means that vehicles can receive information related to traffic safety (such as, collision avoidance, accident report, and warning information) in time, which greatly enhances the traffic safety for the intelligence transportation system. In addition, the proposed IC-SRAA outperforms G-SARR in terms of the average delay, the reason is that the proposed IC-SRAA achieves faster convergence than typically genetic based algorithm, which reduces the average delay and thus contributes to the improvement of safety in the road.

VI. CONCLUSION AND FUTURE WORKS

In this paper, we have focused on the spectrum resource allocation for maximizing the utility of vehicles in LTE-V scenario. Considering both vehicle priority and service priority,

Authorized licensed use limited to: XIDIAN UNIVERSITY. Downloaded on November 30,2020 at 06:31:03 UTC from IEEE Xplore. Restrictions apply.

a two-dimensional service importance evaluation method has been developed. By adopting a graph coloring model, the interference between two adjacent vehicles can be avoided and spectrum resource of cellular base station can be reused at maximum efficiency. We have formulated the spectrum resource allocation problem as a mixed integer programming (MIP) problem combined with the characteristic of stochastic program and proposed a novel IC-SRAA algorithm to solve the MIP problem. Our proposed IC-SRAA would improve the safety in the road because the services with higher priority or vehicles with higher priority would be allocated to more SRBs for the purpose of obtaining the maximal utility in our formulated optimization problem. The real-time services related to traffic safety experience less delay means that vehicles can receive information related to traffic safety (such as, collision avoidance, accident report, and warning information) in time, which greatly enhances the traffic safety for the intelligence transportation system. Moreover, we have proved the convergence of the proposed algorithm theoretically and validated the convergence through numerical simulations. The simulation results have demonstrated that the proposed algorithm achieves faster convergence than typically genetic based algorithm, which also reduces the average delay and thus contributes to the improvement of safety in the road. In addition, the simulation results have shown the significant impact of the number of vehicles, the ratio of SRBs to the number of vehicles and the population size on the achieved system throughput, system utility and spectrum efficiency.

For our future work, it would be interesting to extend our proposal to provide QoS guarantee for each vehicle. And we will jointly consider the power allocation of the cellular base station.

Appendix
Proof of Proposition 1

We define $p_0(g)$ as

$$p_0(g) = p\{\vartheta(\boldsymbol{P}(g)) = 0\} = p\{\boldsymbol{P}(g) \cap B^* \neq \varnothing\}, \tag{32}$$

then according to Bayes' formula, we have

$$\begin{aligned} &p_0(g+1) \\ &= p\{\vartheta(\boldsymbol{P}(g+1)) = 0\} \\ &= p\{\vartheta(\boldsymbol{P}(g+1)) = 0 | \vartheta(\boldsymbol{P}(g)) \neq 0\} p\{\vartheta(\boldsymbol{P}(g)) \neq 0\} \\ &\quad + p\{\vartheta(\boldsymbol{P}(g+1)) = 0 | \vartheta(\boldsymbol{P}(g)) = 0\} p\{\vartheta(\boldsymbol{P}(g)) = 0\}. \end{aligned} \tag{33}$$

According to the definition of $\vartheta(P)$, we have

$$p\{\vartheta(\boldsymbol{P}(g+1)) = 0 | \vartheta(\boldsymbol{P}(g)) \neq 0\} = 0, \tag{34}$$

therefore

$$p_0(g+1) = p\{\vartheta(\boldsymbol{P}(g+1)) = 0 | \vartheta(\boldsymbol{P}(g)) = 0\} p_0(g). \tag{35}$$

We define ξ as

$$\xi = \min_g \vartheta(\boldsymbol{P}(g+1)) \geq 1 | \vartheta(\boldsymbol{P}(g)) = 0, g = 0, 1, 2 \cdots \tag{36}$$

Then we get

$$p\{\vartheta(\boldsymbol{P}(g+1)) \geq 1 | \vartheta(\boldsymbol{P}(g)) = 0\} \geq \xi \ > 0, \tag{37}$$

then we have

$$\begin{aligned} &p\{\vartheta(\boldsymbol{P}(g+1)) = 0 | \vartheta(\boldsymbol{P}(g)) = 0\} \\ &\quad = 1 - p\{\vartheta(\boldsymbol{P}(g+1)) \neq 0 | \vartheta(\boldsymbol{P}(g)) = 0\} \\ &\quad = 1 - p\{\vartheta(\boldsymbol{P}(g+1)) \geq 1 | \vartheta(\boldsymbol{P}(g)) = 0\} \\ &\quad = 1 - \xi < 1. \end{aligned} \tag{38}$$

Therefore,

$$\begin{aligned} 0 \leq p_0(g+1) &\leq (1-\xi) p_0(g) \\ &\leq (1-\xi)^2 p_0(g-1) \\ &\leq \cdots \\ &\leq (1-\xi)^{g+1} p_0(0). \end{aligned} \tag{39}$$

Since the following equations hold

$$\lim_{g \to \infty} (1-\xi)^{g+1} = 0, \tag{40}$$

$$0 \leq p_0(g) \leq 1, \tag{41}$$

Therefore, we have

$$0 \leq \lim_{g \to \infty} p_0(g) \leq \lim_{g \to \infty} (1-\xi)^{g+1} p_0(0) = 0, \tag{42}$$

Therefore, we have the following equation as

$$\lim_{g \to \infty} p_0(g) = 0. \tag{43}$$

Accordingly, we have

$$\begin{aligned} &\lim_{g \to \infty} p\{\boldsymbol{P}(g) \cap B^* \neq \varnothing | \boldsymbol{P}(0) = \boldsymbol{P}_0\} \\ &\quad = 1 - \lim_{g \to \infty} p_0(g) \\ &\quad = 1. \end{aligned} \tag{44}$$

Namely,

$$\lim_{g \to \infty} p\{\vartheta(\boldsymbol{P}(g)) \geq 1 | \boldsymbol{P}(0) = \boldsymbol{P}_0\} = 1. \tag{45}$$

Proposition 1 is thus proved.

References

[1] METIS. (2015). *Mobile and Wireless Communications Enablers for The 2020 Information Society*. Accessed: Jan. 12, 2015. [Online]. Available: www.metis2020.com

[2] T. O. Olwal, K. Djouani, and A. M. Kurien, "A survey of resource management toward 5G radio access networks," *IEEE Commun. Surveys Tuts.*, vol. 18, no. 3, pp. 1656–1686, 3rd Quart., 2016.

[3] S.-Y. Pyun, W. Lee, and D. H. Cho, "Resource allocation for Vehicle-to-Infrastructure communication using directional transmission," *IEEE Trans. Intell. Transp. Syst.*, vol. 17, no. 4, pp. 1183–1188, Apr. 2016.

[4] S. Chen, J. Hu, Y. Shi, and L. Zhao, "LTE-V: A TD-LTE-based V2X solution for future vehicular network," *IEEE Internet Things J.*, vol. 3, no. 6, pp. 997–1005, Dec. 2016.

[5] S. Chen and J. Zhao, "The requirements, challenges, and technologies for 5G of terrestrial mobile telecommunication," *IEEE Commun. Mag.*, vol. 52, no. 5, pp. 36–43, May 2014.

[6] X. Ge, H. Chen, G. Mao, Y. Yang, and S. Tu, "Vehicular communications for 5G cooperative small-cell networks," *IEEE Trans. Veh. Technol.*, vol. 65, no. 10, pp. 7882–7894, Oct. 2016.

[7] S. Chen *et al.*, "Vehicle-to-everything (v2x) services supported by LTE-based systems and 5G," *IEEE Commun. Standards Mag.*, vol. 1, no. 2, pp. 70–76, Jun. 2017.

[8] HUAWEI, Global Mobile Broadband Forum, Hong Kong. (Nov. 2015). *Roans to MBB 2020, Buliding a Better Connected World*. [Online]. Available:h ttp://www.huawei.com/minisite/hwmbbf15/en/lte-v.html

Authorized licensed use limited to: XIDIAN UNIVERSITY. Downloaded on November 30,2020 at 06:31:03 UTC from IEEE Xplore. Restrictions apply.

[9] Y. Zhao, X. Li, X. Zhang, Y. Li, and H. Ji, “Multidimensional resource allocation strategy for high-speed railway MIMO-OFDM system,” in *Proc. IEEE GLOBECOM*, Dec. 2012, pp. 1653–1657.

[10] T. Chen, H. Shan, and X. Wang, “Optimal scheduling for wireless on-demand data packet delivery to high-speed trains,” *IEEE Trans. Veh. Technol.*, vol. 64, no. 9, pp. 4101–4112, Sep. 2015.

[11] J. Li, M. Peng, Y. Yu, and Z. Ding, “Energy-efficient joint congestion control and resource optimization in heterogeneous cloud radio access networks,” *IEEE Trans. Veh. Technol.*, vol. 65, no. 12, pp. 9873–9887, Dec. 2016.

[12] K. Zheng, H. Meng, P. Chatzimisios, L. Lei, and X. Shen, “An SMDP-based resource allocation in vehicular cloud computing systems,” *IEEE Trans. Ind. Electron.*, vol. 62, no. 12, pp. 7920–7928, Dec. 2015.

[13] J. Zhu and K. J. R. Liu, “Cognitive radios for dynamic spectrum access—Dynamic spectrum sharing: A game theoretical overview,” *IEEE Commun. Mag.*, vol. 45, no. 5, pp. 88–94, May 2007.

[14] D. Niyato and E. Hossain, “Competitive pricing for spectrum sharing in cognitive radio networks: Dynamic game, inefficiency of Nash equilibrium, and collusion,” *IEEE J. Sel. Areas Commun.*, vol. 26, no. 1, pp. 192–202, Jan. 2008.

[15] K. Zhu, E. Hossain, and D. Niyato, “Pricing, spectrum sharing, and service selection in two-tier small cell networks: A hierarchical dynamic game approach,” *IEEE Trans. Mobile Comput.*, vol. 13, no. 8, pp. 1843–1856, Aug. 2014.

[16] G. Sun *et al.*, “Coalitional double auction for spatial spectrum allocation in cognitive radio networks,” *IEEE Trans. Wireless Commun.*, vol. 13, no. 6, pp. 3196–3206, Jun. 2014.

[17] S. H. Chun and R. J. La, “Secondary spectrum trading—Auction-based framework for spectrum allocation and profit sharing,” *IEEE/ACM Trans. Netw.*, vol. 21, no. 1, pp. 176–189, Feb. 2013.

[18] H. Huang, Y.-e Sun, X.-Y. Li, S. Chen, M. Xiao, and L. Huang, “Truthful auction mechanisms with performance guarantee in secondary spectrum markets,” *IEEE Trans. Mobile Comput.*, vol. 14, no. 6, pp. 1315–1329, Jun. 2015.

[19] M. Ru, S. Yin, and Z. Qu, “Power and spectrum allocation in D2D networks based on coloring and chaos genetic algorithm,” *Procedia Comput. Sci.*, vol. 107, pp. 183–189, Jan. 2017.

[20] Z. Xu, Y. He, X. Xu, and F. Peng, “QoS graph coloring spectrum allocation for femtocell in Macro/Femto heterogeneous network,” in *Proc. IEEE CHINACOM*, Aug. 2013, pp. 374–378.

[21] W. Wang and X. Liu, “List-coloring based channel allocation for open-spectrum wireless networks,” in *Proc. IEEE VTC*, Sep. 2005, pp. 690–694.

[22] R. Shang, L. Jiao, F. Liu, and W. Ma, “A novel immune clonal algorithm for MO problems,” *IEEE Trans. Evol. Comput.*, vol. 16, no. 1, pp. 35–50, Feb. 2012.

[23] W. Wu, Q. Yang, B. Li, and K. S. Kwak, “Adaptive cross-layer resource optimization in heterogeneous wireless networks with multi-homing user equipments,” *IEEE J. Commun. Netw.*, vol. 18, no. 5, pp. 784–795, Oct. 2016.

[24] Y. Zhang, K. Xiong, F. An, X. Di, and J. Su, “Mobile-service based max-min fairness resource scheduling for heterogeneous vehicular networks,” *China Commun.*, vol. 12, no. s2, pp. 10–18, 2015.

[25] O. B. Karimi, J. Liu, and C. Wang, “Seamless wireless connectivity for multimedia services in high speed trains,” *IEEE J. Sel. Areas Commun.*, vol. 30, no. 4, pp. 729–739, May 2012.

[26] H. Liang and W. Zhuang, “Efficient on-demand data service delivery to high-speed trains in cellular/infostation integrated networks,” *IEEE J. Sel. Areas Commun.*, vol. 30, no. 4, pp. 780–791, May 2012.

[27] W. Wei *et al.*, “Imperfect information dynamic stackelberg game based resource allocation using hidden Markov for cloud computing,” *IEEE Trans. Services Comput.*, vol. 11, no. 1, pp. 78–89, Jan./Feb. 2016.

[28] X. Kang, R. Zhang, and M. Motani, “Price-based resource allocation for spectrum-sharing femtocell networks: A Stackelberg game approach,” *IEEE J. Sel. Areas Commun.*, vol. 30, no. 3, pp. 538–549, Apr. 2012.

[29] Y. Bao, S. Wang, B. Yan, K. Liu, and F. Meng, “Research on maximal weighted independent set-based graph coloring spectrum allocation algorithm in cognitive radio networks,” in *Proc. Int. Conf. Commun., Signal Process., Syst.*, 2016, pp. 263–271.

[30] L. Tan, Z. Feng, W. Li, Z. Jing, and T. A. Gulliver, “Graph coloring based spectrum allocation for femtocell downlink interference mitigation,” in *Proc. IEEE WCNC*, Mar. 2011, pp. 1248–1252.

[31] W. Guo and X. Huang, “Multicast communications in cognitive radio networks using directional antennas,” *Wireless Commun. Mobile Comput.*, vol. 15, no. 2, pp. 260–275, 2015.

[32] Y. Liu, X.-G. Xia, and H. Zhang, “Distributed space-time coding for full-duplex asynchronous cooperative communications,” *IEEE Trans. Wireless Commun.*, vol. 11, no. 7, pp. 2680–2688, Jul. 2012.

[33] H. Peng *et al.*, “Resource allocation for cellular-based inter-vehicle communications in autonomous multiplatoons,” *IEEE Trans. Veh. Technol.*, vol. 66, no. 11, pp. 11249–11263, Dec. 2017.

[34] L. Venturino, N. Prasad, and X. Wang, “Coordinated scheduling and power allocation in downlink multicell OFDMA networks,” *IEEE Trans. Veh. Technol.*, vol. 58, no. 6, pp. 2835–2848, Jun. 2009.

[35] J. Chen *et al.*, “Service-oriented dynamic connection management for software-defined internet of vehicles,” *IEEE Trans. Intell. Transp. Syst.*, vol. 18, no. 10, pp. 2826–2837, Oct. 2017.

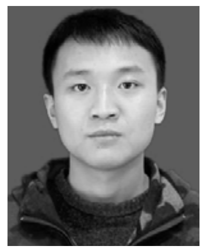

Quyuan Luo received the B.E. degree from Changchun University of Science and Technology, Changchun, China, in 2011. He is currently pursuing the Ph.D. degree in communication and information system with Xidian University, Xi’an, China. His current research interests include intelligent transportation systems, content distribution, and resource allocation in vehicular networks.

Changle Li (M’09–SM’16) received the Ph.D. degree in communication and information system from Xidian University, China, in 2005. He conducted his post-doctoral research in Canada and the National Institute of information and Communications Technology, Japan, respectively. He had been a Visiting Scholar with University of Technology Sydney. He is currently a Professor with the State Key Laboratory of Integrated Services Networks, Xidian University. His research interests include intelligent transportation systems, vehicular networks, mobile ad hoc networks, and wireless sensor networks.

Tom H. Luan (M’10) received the B.E. degree from Xi’an Jiaotong University, Xi’an, China, in 2004, the M.Phil. degree from The Hong Kong University of Science and Technology, Hong Kong, in 2007, and the Ph.D. degree from University of Waterloo, Waterloo, ON, Canada, in 2012. He was a Lecturer with the School of Information Technology, Deakin University, Burwood, VIC, Australia, from 2013 to 2017. He is currently a Professor with the School of Cyber Engineering, Xidian University. His current research interests focus on the content distribution in vehicular networks, mobile cloud computing, and fog computing.

Yingyou Wen received the Ph.D. degree in computer science from Northeastern University, Shenyang, China, in 2005. He was a Post-Doctoral Research Fellow with the Neusoft Group from 2005 to 2008. He is currently an Associate Professor with the School of Computer Science and Engineering, Northeastern University. He is also the Associate Director of the Chinese State Key Laboratory of Software Architecture and the Vice President of the Neusoft Group Research. His research interests include wireless communication and sensor network.

Authorized licensed use limited to: XIDIAN UNIVERSITY. Downloaded on November 30,2020 at 06:31:03 UTC from IEEE Xplore. Restrictions apply.